

# Experimental Identification of Modal Identity-Related Parameters of a Spacecraft Representative Structure

F. R. Vigneron,\* R. K. Singal,\* and Y. Soucy†  
*Canadian Space Agency, Ottawa, Canada*

Modal momentum coefficients and modal identity parameters can, in principle, be identified experimentally using a procedure that entails obtaining estimates of modal momentum coefficients  $\times$  scale factor for each mode from driven-base test data, then obtaining modal scale factors from tests with a portable exciter, and, finally, calculating the modal momentum coefficients from the various estimates. The estimated modal momenta can further be used with modal identities to assess the relative importance of modes and the completeness of the set of identified modes. The results of laboratory tests aimed at assessing the practicality of the procedure in the case of a complex structure are presented. The test structure, called FLECS, is representative of a typical modular spacecraft in terms of mass properties and modal density. The results demonstrate that the procedure successfully identifies the modal parameters.

## Introduction

THE theoretical development in Ref. 1 describes how modal momentum coefficients and modal identity parameters can be identified experimentally by combining measured data from driven-base and portable exciter modal tests. These parameters are obtained in addition to the more conventional modal parameters, namely, frequencies, damping ratios, mode shapes, and modal masses. The theoretical procedure comprises the following: 1) estimates of modal momentum coefficients  $\times$  scale factor for each mode are obtained from driven-base test data; 2) the scale factors are obtained from tests with a portable exciter(s); 3) then estimates of the modal momentum coefficients are calculated from the results of steps 1) and 2). The estimated modal momenta can also be used in conjunction with modal identities to assess the relative importance of experiment-derived modes and the completeness of the set of identified modes. The concepts have been successfully demonstrated by computer simulation of a structure and with test data of a simple cantilever beam in Refs. 1 and 2, respectively. The reader is further referred to these references for additional background and related progress.

This paper presents the results of laboratory work aimed at validating the practicality of the procedure for a complex structure. The structure chosen for the exercise was the FLECS test structure, which is representative of a typical spacecraft in terms of mass properties and modal characteristics. The FLECS structure was provided by the German Aerospace Research Establishment (DLR) through the courtesy of European Space Research and Technology Center (ESTEC), for a project which is part of a cooperative agreement for structural dynamics research between DLR and the Department of Communications of Canada.

## Concepts and Procedures for Modal Parameter Estimation

In the driven-base modal test, the structure under test is either attached to a rigid slip table that is driven horizontally

by a powerful exciter system, or it is mounted on the exciter itself (sometimes through a head expander) for vertical vibration. The input measurement is made with accelerometers mounted to the moving base, and the measured outputs are accelerations at several points on the structure. The more familiar conventional modal test with portable exciters involves fixing the structure to a fixed base, measured inputs that are forces, and outputs that are accelerations.

The theory and assumptions underlying the modeling and corresponding parameter estimation for driven-base and modal survey tests are presented in detail in Ref. 1. A summary outlining the concepts and notation to the extent necessary to support the description of the experimental work of later sections is given in the Appendix. The driven-base test configuration with translational excitation in the  $x$  direction provides data that enable the estimation of the following modal parameters for each mode: natural frequency, damping ratio, mode shape, the product  $Q_k P_{xk}$ , where  $Q_k$  and  $P_{xk}$  are, respectively, the modal normalization constant and linear modal momentum coefficient (i.e., the first moment of the mode shape) in the  $x$  direction, of a  $k$ th mode. A modal test with a portable exciter and a small number of accelerometers (referred to herein as a "partial" modal test) suffices to estimate the  $Q_k$ , provided that the excitation point is not a node and the corresponding output signal contains a sufficiently high content of response of each mode. With the products

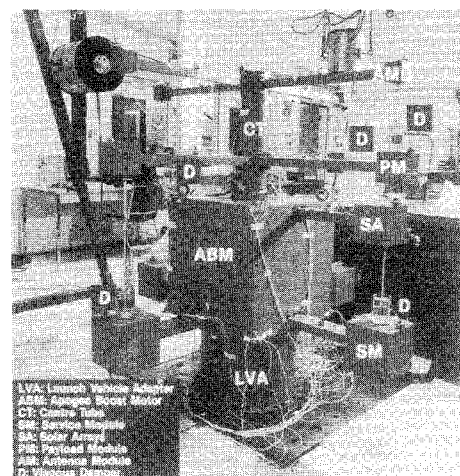


Fig. 1 The FLECS structure, including labeling of its submodules. Also shown are portable exciters used in the modal surveys.

Received March 30, 1989; revision received July 3, 1989. Copyright © 1989 by R. K. Singal. Published by the American Institute of Aeronautics and Astronautics, Inc., with permission.

\*Graduate Research Assistant, Department of Aerospace Engineering and Engineering Mechanics.

†Professor, Department of Aerospace Engineering and Engineering Mechanics.

\*Research Scientist, Directorate of Space Mechanics.

†Research Engineer, Directorate of Space Mechanics.

**Table 1 Description of natural modes of FLECS**

Mode no.	Frequency (Hz)	Module	Type of vibratory motion
1	22.92	CB	1st bending along X
2	23.04	CB	1st bending along Y
3	25.52	CB	1st torsion about Z
4	27.85	SA	4 beams, lat. antisym
		AM	4 beams, lat. antisym
5	28.34	AM	2 beams along Y, lat. sym
		SA	2 beams, lat. sym (oppos. dir)
5a	28.33	CB	bending
		AM	4 beams, lat. sym
6	28.63	AM	4 beams, lat. antisym
7	29.29	AM	2 beams along X, lat. sym
8	29.68	AM	2 beams along Y, lat. sym
		SA	2 beams, lat. sym
		SM	2 beams along X, axial antisym
9	30.76	AM	2 beams along Y, lat. sym
			2 beams along X, axial antisym
		PM	2 beams along X, axial antisym
		SM	2 beams along X, axial sym
10	30.99	AM	2 beams along X, lat. sym
			2 beams along Y, axial antisym
11	30.95	PM	2 beams along Y, axial antisym
		SM	4 beams, axial sym
		PM	4 beams, axial antisym
12	31.33	SM	4 beams, axial sym (oppos. dir)
13	34.81	PM	4 beams, axial sym (oppos. dir)
14	34.70	AM	2 beams along Y, axial antisym
15	36.06	PM	4 beams, axial sym
		AM	2 beams along X, axial sym
			2 beams along Y, axial antisym
16	35.42	PM	4 beams, axial sym
		SA	2 beams, axial antisym
		CB	1st bending along Y
		SM	2 beams along Y, axial antisym
		AM	4 beams, axial antisym
17	35.86	AM	4 beams, axial sym (oppos. dir)
18	36.28	AM	4 beams, axial sym
19	37.86	SA	2 beams, axial sym
20	39.66	CB	2nd torsion about Z
21	39.70	CB	1st beam along X
		AM	2 beams along X, axial antisym
			2 beams along Y, lat. sym
		PM	2 beams along X, axial antisym
		SA	2 beams, lat. sym
		SM	2 beams along X, axial antisym
22	40.56	CB	1st bending along Y
		SA	2 beams, axial antisym
23	49.47	CB	3rd torsion about Z
24	60.37	CB	2nd bending along Y
24a	61.97	CB	axial
25	64.91	CB	2nd bending along X
26	66.48	PM	4 beams, lat. antisym
27	66.79	SM	2 beams along X, lat. antisym
			2 beams along Y, lat. sym
		PM	2 beams along Y, lat. sym (oppos. dir)
28	80.38	PM	2 beams along X, lat. sym
29	81.70	PM	2 beams along Y, lat. sym
		CB	1st bending along X
29a	85.21	CB	axial

$Q_k P_{xk}$  estimated from data of a driven-base test, and the  $Q_k$  estimated from a partial modal test, it is possible to construct estimates of  $P_{xk}$  by dividing  $Q_k P_{xk}$  by  $Q_k$ . These measurement-derived  $P_{xk}$  and  $Q_k$  can further be used to calculate estimates of modal quantities that are associated with modal identities for damped natural modes, and such modal identity parameters can be used to assess the relative significance of individual modes and the overall completeness of the experimental modal determination. Driven-base tests in the  $y$  and  $z$  direction similarly provide for modal parameters corresponding to the  $y$  and  $z$  directions, respectively.

## Experimental Results

### Test Structure

FLECS (Flexible ECS-type Structure) is shown in Fig. 1. It was designed and manufactured by ESTEC, and represents the modular construction of the ECS-type spacecraft MAROTS in terms of mass properties and modal density. The structure has been used in other programs and is well-documented,<sup>3</sup> and is thus well-suited for the evaluation of identification methods. FLECS consists of 1) a center body (CB) composed of cylindrical shell representing a Launch Vehicle Adapter (LVA), a cube representing an Apogee Boost Motor (ABM), and a center tube (CT); 2) four beams with end masses representing the service module (SM) attached to the lower end of the cube; 3) two beams with end load representing the solar arrays (SA) attached to the upper end of the cube; 4) payload module (PM), represented by four beams with end masses, attached to the lower end of the center tube; and 5) antenna module (AM), represented by four top beams with end masses, attached to the center tube. FLECS has a total mass of 929 kg, and an overall height and width of 1.53 m and 1.59 m, respectively. The configuration of FLECS for the present work has five viscous dampers of star-type piston design integrated into it, as may be observed in Fig. 1.

### Modal Frequencies and Shapes

Modal surveys that determined the number of modes, modal frequencies, mode shapes, and damping factors, were done on FLECS in related activities,<sup>4</sup> using the phase resonance method, the mode separation method with portable exciters, and with driven-base excitation. The surveys show that FLECS has 32 modes in the frequency range of 0–112 Hz. In Table 1, a description of each mode is given for later reference, in terms of the type of motion of each module. The mode shapes of FLECS were observed to be in three different categories: 1) modes characterized mainly by motion caused by significant deformation of the center body (CB); 2) modes characterized by isolated motion of individual beams with end masses; and 3) combined motion of center body and one or more of the beam modules. Despite the addition of discrete viscous dampers, the measured damping factors were small and ranged from 0.15% to 3.43%.

### Driven-base and Portable Exciter Tests

Driven-base tests in which the structure was excited sequentially in three orthogonal directions (labeled  $X$  and  $Y$  for the horizontal plane and  $Z$  for the vertical direction) were done for modal parameters determination. For the horizontal directions, the structure was mounted on a rigid slip table through an adapter plate, as is shown in Fig. 2. The slip table was

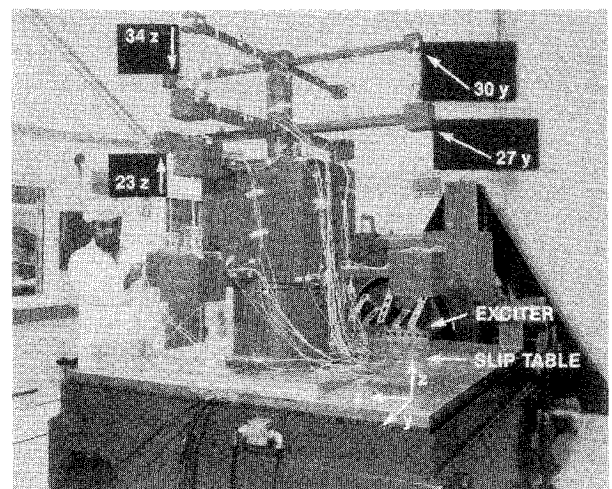


**Fig. 2 The FLECS structure undergoing driven-base tests. Also shown are locations of modal survey driving points.**

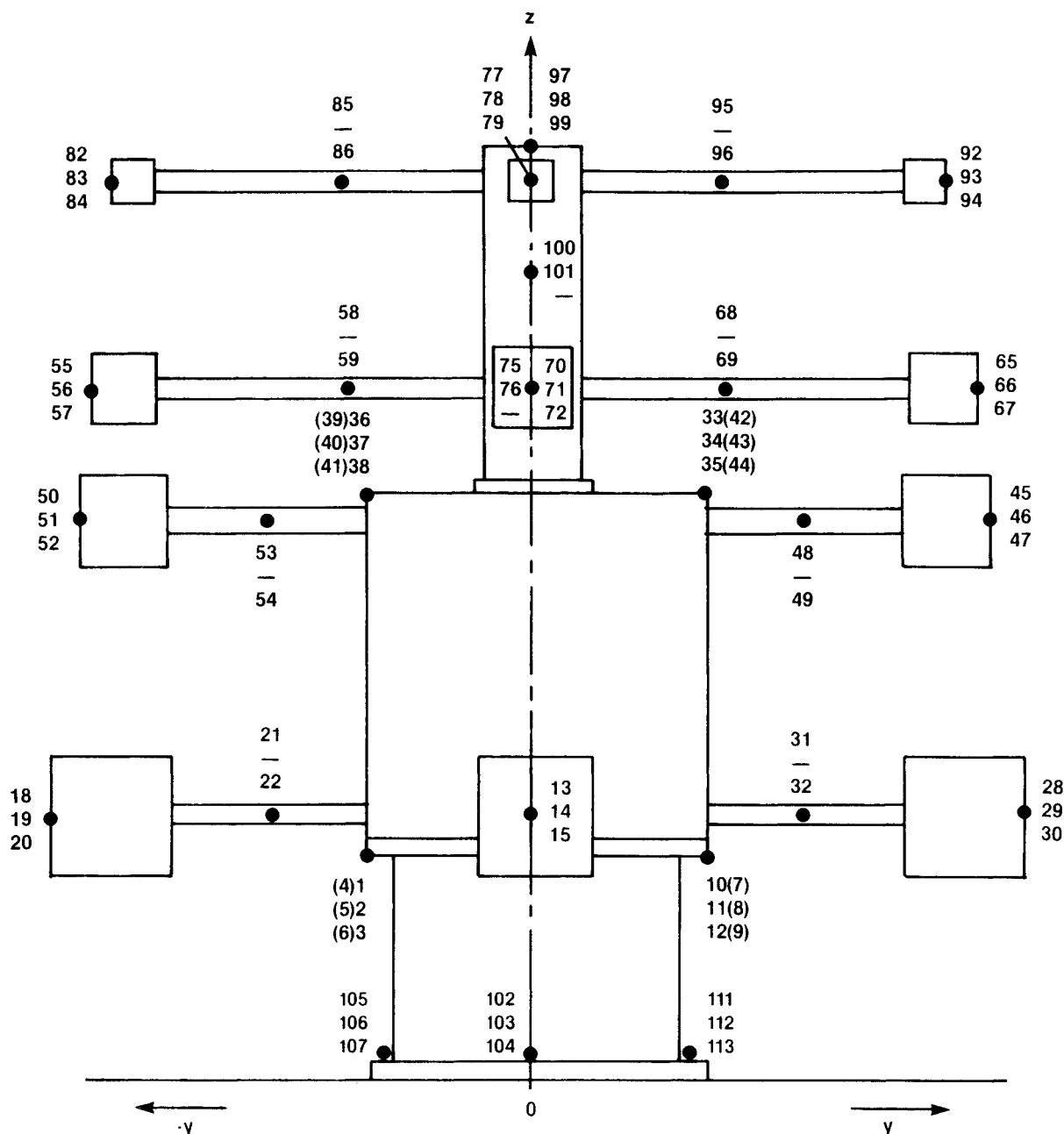


Fig. 3 Measurement point plan.

driven by a 178 kN (40,000 lbf) base exciter. For the vertical excitation, FLECS and its adapter plate were mounted on the exciter through a head expander. For response measurement, 101 accelerometers were mounted on FLECS. They were attached to the structure at 39 measuring points. Figure 3 shows the degree to which the structure was instrumented. In the figure (in the Y-Z plane), next to each measuring point, the corresponding numbers of the transducers are listed in the sequence x, y, z of their individual sensing directions. A horizontal line indicates that a specific component of acceleration was not measured at this point. Numbers in the parenthesis belong to those points which are situated on the opposite side of the structure just behind the visible one. Besides these 101 transducers, 12 more were fixed to the LVA ring at the base of the structure; an additional number (22 in the case of horizontal excitation and 12 in the case of vertical excitation) were mounted to the base to measure its flexibility.

Since FLECS has a high modal density in the frequency range of interest, zoom data were acquired in nine different bandwidths: 22–30 Hz, 28–34 Hz, 32–40 Hz, 38–49 Hz, 48–60

Hz, 58–70 Hz, 67–81 Hz, 79–95 Hz, and 92–112 Hz. The driven-base tests identified all modes of Table 1, except modes 14, 15, and 20. Three modes (labeled 5a, 24a, and 29a) were isolated only with driven-base excitation (Z direction). Mode 5a can be described as a combination type with motion of CB and AM modules. Modes 24a and 29a are of longitudinal type involving deformation of the lower part of the center body (LVA). Figure 4 shows typical mode shapes from driven-base modal surveys.

For the conventional mode separation method with the portable exciters (hereafter called modal survey), it was found that a minimum of two exciters were needed simultaneously to sufficiently excite most of the modes of the structure. Two different surveys were performed with exciter locations, as depicted in Fig. 2. In the first and main survey, the two exciters were located at 30Y and 34Z-, and the responses of 101 accelerometers mounted on the structure were measured. In addition, as mentioned previously, 12 more were fixed on the LVA ring at the base to monitor the boundary conditions. This survey was also the main basis for comparison work

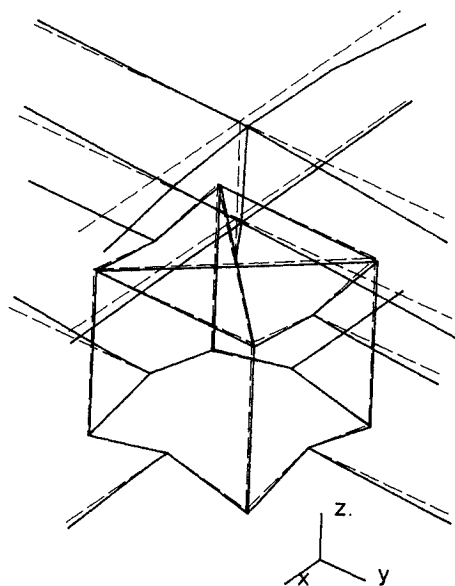


Fig. 4a Mode 2: CB bending mode in  $Y$ ,  $f = 23.04$  Hz.

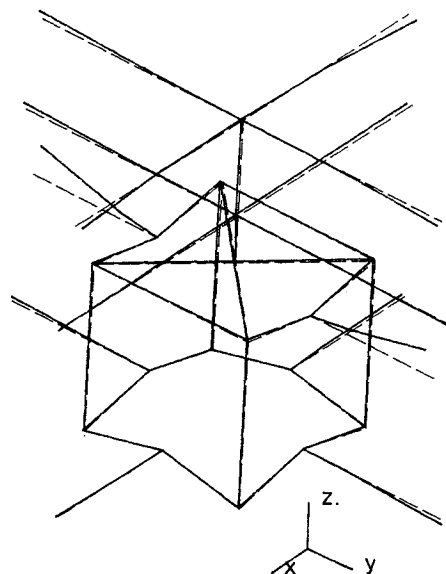


Fig. 4b Mode 19: SA axial bending mode,  $f = 37.86$  Hz.

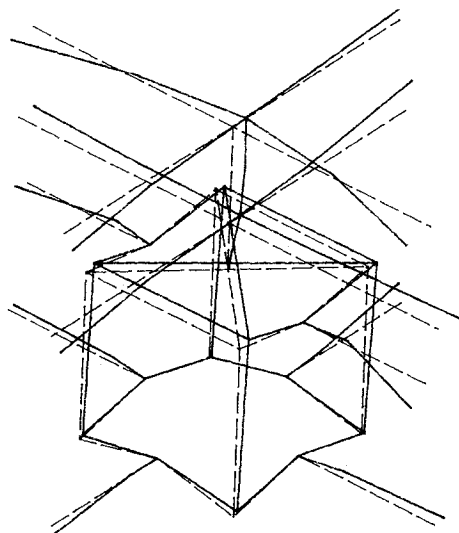


Fig. 4c Mode 21: Combination mode of CB and all beam modules,  $f = 39.70$  Hz.

reported in Ref. 4. A second modal survey was performed with simultaneous excitation at 23Z and 27Y to ensure complete data for the estimation of modal identity parameters. For this second survey, responses of 35 accelerometers were monitored. For both of these surveys, the structure was excited simultaneously with random signals from the two exciters. In the data acquisition phase, the multi-input capability of the FMON software of Leuven Measurement and Systems (LMS) was used, and zoom data were acquired in the nine bandwidths described in the previous paragraph.

The natural frequencies of the modes obtained from the various test configurations are shown in Table 2. The frequencies of Table 1 are taken from Table 2 and correspond to best estimate of mode shapes from driven-base tests. As seen in Table 2, modes 14, 15, and 20 were not obtained from driven-base tests. The salient observations are that no single configuration provides for an estimate of all of the modes, and that there are slight variations in frequency, depending on the configuration.

Two modes were identified through the use of base mounted accelerometers that were attributable to the nonrigidity of the slip-plate system. One such mode is depicted in Fig. 5. In this case, FLECS moves in concert with the base in a rocking rigid-body pattern. The mode is clearly not a structural mode of FLECS, but rather a spurious mode relative to the desired set of structural fixed-base modes, and is not included in Table 2.

The largest differences between frequency estimates from driven-base and portable exciter tests are observed for modes involving deformations of the center body. The small frequency differences between these two configurations can be attributed to a difference in the boundary conditions at the base. The deformations of the base and perturbations to the assumed uniaxial driven-base excitation that were measured with the base-mounted accelerometers were minor for the modes in Table 2.

The residues at the four reference points (23Z, 27Y, 30Y, and 34Z-) for the driven-base and modal survey tests were obtained from the data using the LMS SMAP software, and

Table 2 Natural frequencies of FLECS, Hz

Mode No.	X	Driven-base Y	Z	Portable exciters, 30Y, 34Z-	Portable exciters, 27Y, 23Z
1	22.92	22.92	—	23.81	23.83
2	23.04	23.04	—	24.14	24.25
3	25.47	25.52	—	25.80	25.85
4	27.85	27.91	27.11	27.00	28.00
5	28.34	—	27.91	28.53	28.55
6	28.63	28.65	28.73	28.71	28.80
7	29.41	29.28	—	29.51	29.61
8	29.67	29.78	29.68	29.96	29.96
9	30.94	30.69	30.76	30.95	30.91
10	—	—	30.99	31.08	31.14
11	30.80	30.95	31.31	31.23	31.33
12	31.46	31.33	31.42	31.66	31.73
13	—	35.27	34.81	35.10	35.09
14 <sup>a</sup>	—	—	—	—	—
15	—	—	—	—	36.06
16	—	35.42	35.67	35.89	35.87
17	35.89	35.86	35.88	35.81	36.02
18	36.30	36.27	36.28	36.33	36.43
19	38.69	37.86	—	38.47	38.45
20	—	—	—	39.66	39.59
21	39.70	—	—	41.04	40.91
22	39.87	40.56	—	41.60	41.58
23	51.00	50.70	49.47	51.92	51.65
24	61.61	61.86	60.37	64.67	—
25	64.91	64.64	65.93	66.57	—
26	67.48	—	66.48	67.12	66.69
27	—	66.79	—	70.94	—
28	80.38	80.09	80.88	83.73	83.13
29	81.70	81.82	—	85.88	85.57

<sup>a</sup>Obtained only by phase resonance method.

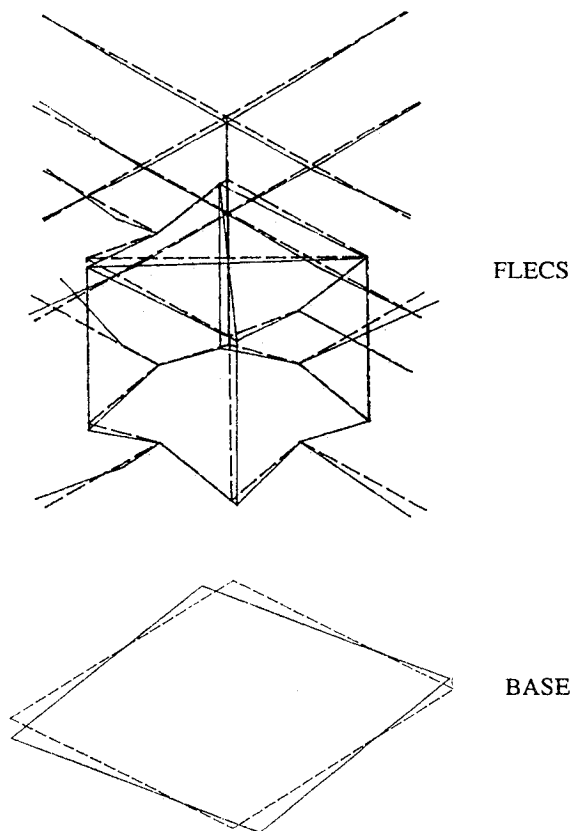


Fig. 5 Example of mode attributable to flexibility of driven-base mounting (excitation in vertical direction),  $f = 61.97$  Hz.

from them estimates of  $Q_k$ ,  $Q_k P_{yk}$ ,  $Q_k P_{zk}$ ,  $P_{yk}$ , and  $P_{zk}$  were calculated. It is particularly noteworthy that the derivation of the residues was found to be a rather complex topic in practice, in spite of being straightforward in theory. A substantial amount of background investigation was involved in refining procedures to obtain confident estimates of the residues, particularly in the case of closely spaced modes from driven-base excitation configuration.

The estimates of  $Q_k P_{yk}$ ,  $Q_k$ ,  $P_{yk}$ , for driving point 27Y are given in Table 3. It is observed that these estimates are complex-valued. The  $Q_k P_{yk}$  are residues at the driving point location from driven-base test in Y direction, and  $Q_k$  are residues at the same location from the portable exciter test. Estimates of  $P_{yk}$  can be obtained only if estimates of both  $Q_k P_{yk}$  and  $Q_k$  are measured.

For certain modes, the phase estimates of  $Q_k P_{yk}$  were close to 0 deg or 180 deg (instead of being close to 90 deg or -90 deg). This usually occurred with closely spaced modes and it indicates that the estimation algorithm was unable to isolate adequately the mode with the given data set from driven-base excitation. The shortcoming in estimating some reliable driven-base residues is believed to be associated with a general observation that separation of multiple (or very closely spaced) modes necessitates simultaneous processing of responses from multiple inputs. The driven-base data are essentially single input data.

The most interesting parameters are the  $M^k$  values. The residues at the four different driving points for the modal surveys in conjunction with the residues at these same points for the three uniaxial driven-base tests enable up to four independent estimates of each of  $M_{xx}^k$ ,  $M_{yy}^k$ , and  $M_{zz}^k$  to be obtained.

#### Estimates of $M_{yy}^k$

The estimates of  $M_{yy}^k$  for each mode and their sums are presented in Table 4. For a particular mode (row), the estimates are independent and in theory should be equal and four

Table 3 Estimates of momentum coefficient related parameters for FLECS from the reference point 27Y

Mode no.	$Q_k P_{yk}$ , s		$Q_k$ , s/kg		$P_{yk}$ , kg	
	Ampl.	Phase	Ampl.	Phase	Ampl.	Phase
1	0.866E-3	175.5	0.131E-6	-95.7	6621.0	-88.2
2	0.242E-2	61.9	0.295E-5	-93.8	820.0	155.7
3	0.362E-4	119.6	0.336E-5	-86.9	10.8	206.5
4	—	—	0.107E-7	-79.3	—	—
5	—	—	0.166E-7	-108.3	—	—
6	—	—	—	—	—	—
7	0.638E-4	82.3	0.256E-6	-73.7	249.0	156.0
8	—	—	—	—	—	—
9	0.107E-4	101.3	—	—	—	—
10	—	—	—	—	—	—
11	—	—	—	—	—	—
12	0.348E-4	135.8	—	—	—	—
13	0.423E-3	74.8	—	—	—	—
14	—	—	—	—	—	—
15	—	—	—	—	—	—
16	0.497E-3	102.9	—	—	—	—
17	—	—	—	—	—	—
18	—	—	—	—	—	—
19	0.217E-3	92.9	—	—	—	—
20	—	—	0.134E-4	-84.6	—	—
21	—	—	—	—	—	—
22	0.146E-2	76.4	0.355E-5	-87.0	410.0	163.4
23	0.207E-4	-89.1	0.137E-4	-91.8	1.51	2.7
24	0.193E-3	-111.0	—	—	—	—
25	0.693E-4	-145.9	—	—	—	—
26	—	—	0.198E-4	-89.9	—	—
27	0.631E-4	-113.6	—	—	—	—
28	0.730E-3	-93.7	0.285E-4	-87.9	25.6	-5.8
29	0.597E-4	-71.9	0.616E-6	-91.4	96.8	19.4

in number. Such is not quite the case with the real data given in Table 4.

For several modes, there is no estimate in columns 2 to 5. As mentioned before for  $P_{yk}$ , this corresponds to situations where no measurement of the mode is available at that location, either for the driven-base modal test or for the modal survey, or for both, in which case it is not possible to calculate  $M_{yy}^k$  for that mode from the corresponding response location. This situation occurs if the reference point is on a part of the structure which is not well-excited in that mode, or is at a node.

In Table 4, the "Best Estimate" (sixth column) for a particular mode is obtained by averaging acceptable estimates from the corresponding reference points. Estimates with no superscript are of high confidence. For mode 1, for example, the estimates from 23Z and 34Z- are generated from data with good signal/noise and good curve fit characteristics, and correlate with each other in magnitude; they are, thus, confident estimates. The superscript 'b' indicates that the corresponding estimate is not reliable and, consequently, was not used in the best estimate computation for that mode. Values were considered unreliable if one or both residues ( $Q_k P_{yk}$  and  $Q_k$ ) used in their calculation were believed inaccurate. The inaccuracy was assumed if one or more of the following conditions was experienced: 1) mode was not well-defined, as indicated by a frequency response function having no or almost invisible peak, poor phase shift (for isolated mode); 2) a poor curve fit was obtained; 3) an estimated phase value was obtained which was closer to 0 deg or 180 deg instead of  $\pm 90$  deg. The presence of superscript 'a' in Table 4 indicates that the estimate is believed to be an acceptable, but not fully reliable, approximation of  $M_{yy}^k$ . In these cases, a fully reliable estimate was not available for the mode.

The best estimates of Table 4 are consistent in every case with a qualitative physical interpretation of them, derived by considering the mode description of Table 1. As would be expected, modes 2 and 22 have the largest values of  $M_{yy}^k$ , as they involve the first bending along Y, for which the whole center body (having 50% of the mass of FLECS) moves in one

Table 4  $M_{yy}^k$  for FLECS, kg

Mode no.	Reference point				Best est.
	23 Z	27 Y	30 Y	34 Z-	
1	58.0	1715.0 <sup>b</sup>	34.4 <sup>b</sup>	53.1	55.5
2	2267.0 <sup>b</sup>	370.7	230.2 <sup>b</sup>	368.9	369.8
3	—	0.07 <sup>b</sup>	0.02 <sup>b</sup>	—	—
4	0.001	—	0.02 <sup>b</sup>	0.002	0.0
5	—	—	—	—	—
6	—	—	0.03	—	0.0
7	—	5.04 <sup>b</sup>	8.15	—	8.2
8	0.001	—	—	—	0.0
9	0.03	—	—	—	0.0
10	—	—	—	—	—
11	1.08 <sup>a</sup>	—	—	0.8 <sup>a</sup>	0.9
12	—	—	—	—	—
13	-33.0 <sup>b</sup>	—	—	-4.2 <sup>b</sup>	—
14	—	—	—	—	—
15	—	—	—	—	—
16	44.2 <sup>b</sup>	—	—	17.9 <sup>b</sup>	—
17	0.05 <sup>b</sup>	—	—	0.1 <sup>a</sup>	0.1
18	-1.02 <sup>b</sup>	—	—	-0.07 <sup>b</sup>	—
19	—	—	—	—	—
20	—	—	—	—	—
21	—	—	—	—	—
22	—	270.6	332.8 <sup>b</sup>	—	270.6
23	—	0.02 <sup>a</sup>	—	—	0.0
24	—	—	—	—	—
25	—	—	—	—	—
26	—	—	—	—	—
27	—	—	—	—	—
28	—	19.3	—	—	19.3
29	—	4.9 <sup>a</sup>	—	—	4.9
$\Sigma M_{yy}$					729.4
Total mass of FLECS					929.0

<sup>a</sup>Estimate of moderate confidence, used for best estimate calculation.<sup>b</sup>Low-confidence, not used for best estimate computation.

direction. One can observe that the  $M_{yy}^k$  estimates for the torsion and the antisymmetric modes (such as numbers 3, 6, and 23) are generally small. This is rational, since FLECS is symmetric with respect to its main axes. For a perfectly symmetric structure, the  $M_{yy}^k$  values would be zero for these two types of modes, since the linear momentum contribution of each part of the structure would cancel the linear momentum of the corresponding part moving in the opposite direction with the same velocity. For modes that contain predominant motion not in the Y direction, the associated  $M_{yy}^k$  values are generally small. Modes 8 and 19 are good examples of this situation.

The summation of the  $M_{yy}^k$  over the frequency range from zero to infinity is, in theory, equal to the mass of the structure. In this practical situation, the summation for the frequency range of 0–112 Hz is 729 kg, which represents about 79% of the mass (929 kg). The summation and its elements are believed to be complete and reliable for the Y-axis estimations. The unidentified 21% of the mass is believed to be associated with modes outside the frequency range of the tests (i.e., above 112 Hz).

#### Estimates of $M_{xx}^k$

The estimates of  $M_{xx}^k$  for each mode and their sums are presented in Table 5. The estimates were derived from four independent reference points in a manner parallel to that described in the preceding subsection.

The largest  $M_{xx}^k$  (418.0) is the one corresponding to the first bending mode and has a value that corresponds to 45% of the mass of the structure. This value is larger than the one associated with the similar bending mode along the Y direction (369.8, Table 4); this is explained by the orientation of the solar array beam modules in the Y direction. The other two large values of  $M_{xx}^k$  (modes 5 and 29) are for lateral symmetric motion along the X direction.

Table 5  $M_{xx}^k$  for FLECS, kg

Mode no.	Driving point				Best est.
	23 Z	27 Y	30 Y	34 Z-	
1	419.0	307.0 <sup>b</sup>	20.3 <sup>b</sup>	417.0	418.0
2	—	16.4 <sup>b</sup>	2.85 <sup>b</sup>	—	—
3	—	0.017	0.014	—	0.0
4	2.04	—	1.90	1.63 <sup>b</sup>	1.8
5	31.5	—	—	23.2 <sup>b</sup>	31.5
6	—	—	0.13	—	0.1
7	—	-0.07 <sup>b</sup>	-0.05 <sup>b</sup>	—	—
8	-10.9 <sup>b</sup>	—	—	—	—
9	0.49	—	—	—	0.5
10	—	—	—	—	—
11	-0.09 <sup>b</sup>	—	—	0.01 <sup>b</sup>	—
12	—	—	—	—	—
13	—	—	—	—	—
14	—	—	—	—	—
15	—	—	—	—	—
16	—	—	—	—	—
17	0.12 <sup>a</sup>	—	—	—	0.1 <sup>a</sup>
18	0.23	—	—	0.16 <sup>b</sup>	0.2
19	—	—	—	—	—
20	—	—	—	—	—
21	—	23.4 <sup>b</sup>	—	7.94 <sup>a</sup>	7.9 <sup>a</sup>
22	—	9.51	—	9.59	9.6
23	—	—	—	—	—
24	—	—	—	—	—
25	—	0.11 <sup>a</sup>	—	—	0.1 <sup>a</sup>
26	—	—	—	—	—
27	—	—	—	—	—
28	—	0.75 <sup>a</sup>	—	—	0.7 <sup>a</sup>
29	—	30.09 <sup>a</sup>	—	—	30.1 <sup>a</sup>
$\Sigma M_{xx}$					500.6
Total mass of FLECS					929.0

<sup>a</sup>Estimate of moderate confidence, used for best estimate calculation.<sup>b</sup>Low-confidence, not used for best estimate computation.

The summation of the  $M_{xx}^k$  is 501 kg, which represents only 54% of the mass of FLECS. A certain amount of the 46% unaccounted for is associated with modes above 112 Hz, which were not measured. However, for data of this axis (X), some of the unaccounted summation is believed attributable to poor or missing estimates of  $M_{xx}^k$  in the frequency range 0–112 Hz.

The poor and/or missing estimates in this case are due to shortcomings in placement and orientation of the reference point exciters. For example, one element of mode 9 is lateral symmetric motion of the two AM beams aligned along the Y-axis direction. Although measurements from the driven-base and modal survey tests produce good mode shapes, the estimated  $M_{xx}^k$  of 0.49 seems to be too small. The shortcoming is that the residues at the driving (reference) point location were not well-defined (even though the excitation produced measurable motions at many other points); at least one reference point should have been chosen on one of the two AM beams in order to obtain adequately measurable signals. Further, it is likely that certain  $M_{xx}^k$  were underestimated for some of the modes because the driving directions at a reference point were not oriented in the direction of major motion.

#### Estimates of $M_{zz}^k$

The main observation from the estimates of  $M_{zz}^k$  in Table 6 is that major  $M_{zz}^k$  seem to be unidentified, since the total sum of all the best estimates is only 159.0 kg, which is only 17% of the mass of the structure. The main reason for this low summation of linear momentum is the fact that Table 6 contains no value corresponding to longitudinal modes of the structure that would involve the whole structure moving in the Z direction.

One of the unidentified modes is the first longitudinal mode of the center body (mode 29a in Table 1). This mode was measured with the Z-axis driven-base excitation, but it was

Table 6  $M_{zz}^k$  for FLECS, kg

Mode no.	23 Z	Reference point			Best est.
		27 Y	30 Y	34 Z-	
1	—	—	—	—	—
2	—	—	—	—	—
3	—	—	—	—	—
4	—	—	0.11	—	0.1
5	1.29	—	—	0.90	1.1
6	—	—	0.0007	—	0.0
7	—	—	—	—	—
8	-27.3 <sup>b</sup>	—	—	—	—
9	40.4 <sup>a</sup>	—	—	—	40.4 <sup>a</sup>
10	—	—	18.2	—	18.2
11	2.64	—	—	2.49	2.6
12	—	—	—	—	—
13	-6.35 <sup>b</sup>	—	—	-2.91 <sup>b</sup>	—
14	—	—	—	—	—
15	—	—	—	—	—
16	146. <sup>b</sup>	—	—	72.7 <sup>a</sup>	72.7 <sup>a</sup>
17	-0.14 <sup>b</sup>	—	—	-0.03 <sup>b</sup>	—
18	23.9 <sup>a</sup>	—	—	15.0 <sup>b</sup>	23.9 <sup>a</sup>
19	—	—	—	—	—
20	—	—	—	—	—
21	—	—	—	—	—
22	—	—	—	—	—
23	—	0.03	—	—	0.0
24	—	—	—	—	—
25	—	—	—	—	—
26	—	0.002	—	—	0.0
27	—	—	—	—	—
28	—	0.040	—	—	0.0
29	—	—	—	—	—
$\Sigma M_{zz}$					159.0
Total mass of FLECS					929.0

<sup>a</sup>Estimate of moderate confidence, used for best estimate calculation.

<sup>b</sup>Low-confidence, not used for best estimate computation.

not captured in the portable exciter modal surveys. To identify this type of mode, it would have been necessary to excite FLECS vertically at the top of the CB module. An other major source of the unidentified  $M_{zz}^k$  is second and higher order longitudinal modes, as well as axial beam modes above the 112 Hz test range.

Another cause for the low summation of the  $M_{zz}^k$  is the underestimation of the linear momenta due to shortcomings of the location of the portable exciters. A good example is mode 11, for which the four SM beams move together in the Z direction, although no exciters were located on these modules.

### Summary and Conclusions

The work of this paper demonstrates that the procedures outlined in the theoretical work of Ref. 1 can be successfully applied in a practical situation with a complex structure to obtain estimates of the modal momenta and identity parameters. However, there are potential pitfalls to be avoided that are noted below.

The choice of portable exciter locations and directions is crucial for obtaining reliable and complete estimates of residues and related momentum coefficients. For each mode of interest, at least one driving point (location and direction) must be chosen, such that substantial measurable motion is induced at the reference (driving) point, especially for the modes that potentially contain a large amount of linear momentum. It was observed with FLECS that if the driving point is not judiciously selected, the residue at the driving point might not be well-defined enough to produce a reliable estimate of  $M^k$ , although a measurable mode shape may be obtained. It was found that a cross-check of independent estimates of the  $M^k$  is very helpful in assessing the reliability of estimates. From the FLECS exercise, it is concluded that the best procedure is to first perform the driven-base test, and then use the driven-base mode shapes for judicious selection

of the driving points for the portable exciter tests done subsequently (this is contrary to what was done for FLECS).

Residues of some closely spaced modes from the driven-base tests could not be identified precisely enough to produce reliable estimates of the  $M^k$ . The unidirectional driven-base test procedures inherently do not provide response functions derived from multi-input data.

Unplanned movements of the base (rotations or deformations) may result in the appearance of modes in addition to the modes of the structure, and/or a slight modification to modes of interest. Although, in theory, the  $\sum_{k=1}^n M^k$  in one direction for all the modes should equal the mass of the structure under test, in practice, the mass of the structure may effectively and inadvertently include an undetermined fraction of the mass of the base fixture. These effects may be detected and assessed by adequately instrumenting and monitoring the driven-base as part of the test exercise.

### Appendix: Theoretical Principles for Experimental Identification of Modal Momentum Coefficients and Related Parameters

A structure undergoing driven-base modal test is illustrated schematically in Fig. A1. The rigid base is assumed driven in a single direction,  $O_x$ , with no rotation. The reference axes ( $O_x, O_y, O_z$ ) are fixed to an arbitrary convenient location of the driven-base. The deformation of each mass point of the structure is defined relative to the driven-base by components ( $u^i, v^i, w^i$ ) in the ( $O_x, O_y, O_z$ ) reference frame. The measurable quantities upon which parameter estimation is based are: 1) the input acceleration,  $a_0(t)$ , equal to  $\ddot{x}(t)$ , and 2) the inertial accelerations at each mass point denoted by  $\{a_x^i(t), a_y^i(t), a_z^i(t)\}$ . The analytical model of this test configuration can be described in the frequency domain by

$$\frac{1}{\omega^2} \begin{bmatrix} \bar{A}_x(\omega)/\bar{a}_0(\omega) - \Sigma \\ \bar{A}_y(\omega)/\bar{a}_0(\omega) \\ \bar{A}_z(\omega)/\bar{a}_0(\omega) \end{bmatrix} = \sum_{k=1}^n \left\{ \frac{Q_k P_{xk} \Phi_k}{i\omega - \lambda_k} + \frac{Q_k^* P_{xk}^* \Phi_k^*}{i\omega - \lambda_k^*} \right\} \quad (A1)$$

In Eq. (A1),  $A_x^T = [a_x^1, a_x^2, \dots, a_x^N]$  and  $\Sigma^T = [1, 1, \dots, 1]$ , and  $A_x, \Sigma$ , etc. are all of order  $N \times 1$ , where  $N$  is the number of mass points of the assumed model for the structure. Also,  $\lambda_k, \Phi_k, Q_k$ , and  $P_{xk}$  are modal parameters of the  $k$ th mode, the mode shape  $\Phi_k$  is of order  $3N \times 1$ , and  $n$  is equal to  $3N$ . A modal eigenvalue,  $\lambda_k$ , is related to its modal frequency,  $\omega_k$ , and damping ratio,  $\zeta_k$ , by  $\lambda_k = -\zeta_k \omega_k + i\omega_k(1 - \zeta_k^2)^{1/2}$ . The  $Q_k$  is the modal normalization constant. The linear modal momentum coefficient  $P_{xk}$  is defined by

$$P_{xk} = \sum_{i=1}^N m^i \theta_k^i \quad (A2)$$

where  $m^i$  is the mass of the  $i$ th point, and  $\theta_k^i$  is the component in the  $O_x$  direction of the  $k$ th mode shape associated with  $m^i$ .

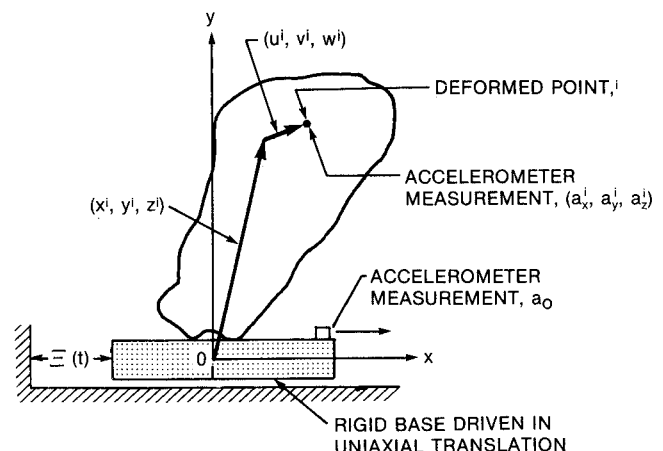


Fig. A1 Schematic of driven-base test configuration.

Note that  $P_{xk}$  might also be described as a first moment of the  $k$ th mode shape about the  $O_x$  axis. The parameters  $Q_k$ ,  $P_{xk}$ ,  $\theta_k$ ,  $\Phi_k$ , and  $\lambda_k$  are complex-valued, and the \* denotes complex conjugate. Equation (A1) relates the modal parameters (right-hand side,  $\lambda_k$ ,  $\Phi_k$ ,  $Q_k$ , and  $P_{xk}$ ,  $k = 1$  to  $n$ ) to the quantities that are directly measurable (left-hand side,  $A$ 's and  $a_0$ ), and is the basic model needed for parameter estimation by curve-fitting methods, for driven-base tests with single-degree-of-freedom excitation in the  $O_x$  direction. Equation (A1) corresponds to a passive structure with general linear viscous (not proportional) damping.

Estimates of the functions  $\bar{A}_x(\omega)/\bar{a}_0(\omega)$ ,  $\bar{A}_y(\omega)/\bar{a}_0(\omega)$ , and  $\bar{A}_z(\omega)/\bar{a}_0(\omega)$  may be obtained from the accelerometer data of a test, using standard data acquisition and spectral analysis equipment. From these quantities, a measurement-based estimate of the functions appearing on the left-hand side of Eq. (A1) may be constructed. Modal parameter estimation then entails determination of the values of the modal parameter set  $\{\lambda_k, \Phi_k, (Q_k P_{xk})\}$  that result in an acceptable curve fit of Eq. (A1) to the measurement-based estimate of the functions.

For the driven-base test, it can be deduced from Eq. (A1) that if the  $k$ th mode shape is normalized so that  $\phi_k^d$  is unity, where  $\phi_k^d$  refers to the  $d$ th component of  $\Phi_k$ , then  $Q_k P_{xk}$  is equal to the residue of the  $d$ th component. There is not enough information to deduce separate estimates of  $Q_k$  and  $P_{xk}$  solely from the data of the driven-base tests.

For a conventional modal survey with a single portable exciter, the corresponding analytical model is

$$-\omega^2 \begin{bmatrix} \bar{A}_x(\omega)/\bar{f}_0(\omega) \\ \bar{A}_y(\omega)/\bar{f}_0(\omega) \\ \bar{A}_z(\omega)/\bar{f}_0(\omega) \end{bmatrix} = \sum_{k=1}^n \left\{ \frac{Q_k \phi_k^d \Phi_k}{i\omega - \lambda_k} + \frac{Q_k^* \phi_k^d \Phi_k^*}{i\omega - \lambda_k^*} \right\} \quad (A3)$$

where  $f_0$  is the reference force input. The modal parameters that are estimated are the set  $\{\lambda_k, \Phi_k, Q_k\}$ . If the  $d$ th location is specified to be the driving point (reference point) and the  $k$ th mode shape is normalized so that  $\phi_k^d$  is unity, then the corresponding residue at the reference point is equal to  $Q_k$ .

Thus, driven-base test with excitation in the  $O_x$  direction provides an estimate of the products  $Q_k P_{xk}$ , and a partial modal survey provides an estimate of  $Q_k$ . It follows that an estimate of the linear modal momenta  $P_{xk}$  can be obtained by dividing the aforementioned two estimates.

A modal identity involving the  $O_x$ -associated linear momentum coefficients may be written in the form

$$\sum_{k=1}^n M_{xx}^k \leq m \quad (A4)$$

where  $M_{xx}^k$  are "modal identity parameters" defined by

$$M_{xx}^k = \lambda_k Q_k P_{xk}^2 + \lambda_k^* Q_k^* P_{xk}^{*2} \quad (A5)$$

Estimates of  $\lambda_k$ ,  $Q_k$ , and  $P_{xk}$  can be derived from tests as outlined in the foregoing and, from them, measurement-based estimates for  $M_{xx}^k$  can be calculated using Eq. (A5). A measure of the net linear momentum,  $M_{xx}^k$ , is associated with the  $k$ th vibratory mode, and is also invariant to the choice of modal normalization constant of  $\Phi_k$ . Comparison of the individual  $M_{xx}^k$ ,  $k = 1, 2$ , etc., gives an indication of the relative linear momentum in the  $x$  direction of each mode. The mass  $m$  of the structure can be estimated by weighing it. Equation (A4) states that the sum of the experimentally derived  $M_{xx}^k$  should equal  $m$ , and the extent to which it does gives an indication of the accuracy of the experimental modal determination process.

Similarly, estimates of  $P_{yk}$ ,  $M_{yy}^k$ , as well as  $P_{zk}$ ,  $M_{zz}^k$ , can be obtained by performing a driven-base test with the excitation in the  $O_y$  and  $O_z$  direction, respectively. Equations corresponding to Eqs. (A4) and (A5) are also available for these two directions.

## Acknowledgments

The FLECS structure was provided by the DLR of Germany through the courtesy of ESTEC of the European Space Agency. The activities with FLECS are part of work associated with cooperative agreement between DLR and the Canadian Department of Communications. The modal tests described herein were supported by the David Florida Laboratory in Ottawa, Canada.

## References

- <sup>1</sup>Vigneron, F. R., and Soucy, Y., "Driven-Base Tests for Modal Parameter Estimation," *AIAA Journal*, Vol. 25, No. 1, 1987, pp. 152-160.
- <sup>2</sup>Soucy, Y., Vigneron, F. R., and Steele, T., "Experimental Identification of Modal Momentum Coefficients and Modal Identity Parameters," *AIAA Journal*, Vol. 27, No. 8, 1989, pp. 1097-1101.
- <sup>3</sup>Nellessen, E., "Design and Verification of the FLECS Test Structure," *ESA Journal*, Vol. 11, No. 3, 1987, pp. 317-341.
- <sup>4</sup>Singal, R. K., Vigneron, F. R., Steele, T., Bertram, A., and Degener, M., "Comparison of Phase Resonance, Mode Separation, and Driven-Base Modal Identification Methods Applied to the FLECS Test Structure," *Proceedings of International Conference on Spacecraft Structures and Mechanical Testing*, Noordwijk, the Netherlands, ESA SP-289, Jan. 1989, pp. 301-308.